Available online at www.sdcjter.in

SDC Journal of Theoretical and Experimental Research (SDCJTER) 01(01), 2023, 31–39

Variability in nightside lunar surface charging with high energy electron fluxes

S.B. Rakesh Chandran [a,b*], S.R. Rajesh[a], A. Abraham [b,c], A.P Sunitha [d], G. Renuka [e], Chandu Venugopal [f]

[a] Department of Physics, Sanatana Dharma College, University of Kerala, Alappuzha, 688 003, Kerala, India.
[b] Department of Physics, University of Kerala, Kariavattom, 695 581, Kerala, India
[c] Christian College, University of Kerala, Chengannur, 689 122, Kerala, India.
[d] Department of Physics, Government Victoria College, Palakkad, Kerala-678001
[e] Department of Physics, University of Kerala, Kariavattom 695 581, Kerala, India (Rtd.)
[f] School of Pure and Applied Physics, M.G. University, Kottayam, 686 560, Kerala, India.

Available online 01 January 2023

Abstract

Our lunar surface is exposed to all kinds of radiations from the Sun, since it lacks a global magnetic field. Like lunar surface, dust particles are also exposed to plasmas and UV radiation and, consequently they carry electrostatic charges. During Solar Energetic Particle events (SEPs) secondary electron emission plays a vital role in charging of lunar dusts. To study the lunar dust charging during SEPs on lunar wake region, we derived an expression for lunar dust potential and analyzed how it varies with different electron temperatures and grain radii. Because of high energetic solar fluxes, secondary yield (δ) values reach up to 2.3 for 0.5 μm dust grain. We got maximum yield at an energy of 550 eV which is in well agreement with lunar sample experimental observation (Anderegg et al., 1972). It is observed that yield value increases with electron energy, reaches to a maximum value and then decreases. During SEPs heavier dust grains show larger yield values because of the geometry of the grains. On the wake region, the dust potential reaches up to -497 V for 0.5 μm dust grain. The electric field of these grains could present a significant threat to manned and unmanned missions to the Moon.

© 2023 Published by Sanatana Dharma College, Alappuzha.

Keywords: SEP events, Lunar dust charging, Lunar surface charging, Secondary electron yield, Dust levitation.

1. **Introduction**

The lunar surface is exposed to solar UV and X - rays as well as solar wind magnetospheric plasma. Its interaction causes the lunar surface to become electrically charged. During Solar Energetic Particles events (SEPs), the night side surface- lunar wake region can reach very large negative potentials because of highly energetic plasma. Earlier we studied the charging mechanism on lunar wake region and obtained a surface potential of -83 V (Rakesh Chandran, Renuka and Venugopal, 2013).

The Moon is covered with powdery soil and rock fragments called the lunar regolith. An average regolith grain size is 70 μm , too fine to observe with the human eye (Stubbs, Vondrak and Farrell, 2006). The dust components from Apollo samples contain grain size as small as 0.01 μm (Colwell et al., 2007). In addition to its size, the lunar dust has a very large surface area that is approximately 8 times that of a sphere of equivalent size (Cain, 2010). Like lunar surface, dust particles also charge in response to the incident currents. Electrostatic charging of lunar surface and dust grains causes the dust to be repelled from the like charged surface. There exists solid observational evidence for the electrostatic transport of charged dust within a few metres of the surface from a variety of sources, including Surveyor (Rennilson and Criswell, 1974) and the Apollo 17 Lunar Ejecta and Micrometeoroids (LEAM) surface experiment (Horanyi, 1998).

* Corresponding author: *Email address*: rakesh@sdcollege.in (Rakesh Chandran S.B)

Lunar dust grains are very often influenced by solar wind plasma and thus they are charged to various potentials. For this reason, the interaction of dust grains with solar wind has been widely studied (Rennilson and Criswell, 1974; Whipple, Northrop and Mendis, 1985; Horanyi, 1996; Colwell et al., 2007). An equilibrium grain potential depends on plasma environment as well as on the size, shape and history. A precise estimation of an equilibrium dust potential in a specific plasma environment can thus be complicated. These charged dusts can levitate above the lunar surface electrostatically and could damage the equipment in the spacecraft and could cause problems by adhering to clothing and equipment, reducing external visibility on landing, etc (Stubbs, Vondrak and Farrell, 2006). Criswell (1973) suggested that horizon glow observed by Surveyor - 7 was caused by electrostatically levitated dust grains with radius 1 μm . The charging mechanism is more complicated during SEPs when the electron energy is very high (Halekas et al., 2008).

The charging of isolated dust particles in plasma were also studied experimentally (Anderegg et al., 1972). During high energy electron fluxes, these experimental results deviate much from existing theoretical models. During SEPs, secondary electron current plays a vital role in charging of dust grains. Most models (Horanyi, 1996) used the Sternglass (1957) theory for calculating secondary electron yield (δ) which is completely independent of grain radius. The theory is good only for planar samples, where the electrons are assumed to escape from only one surface- the side at which the primary electrons enter. For a spherical dust grain, secondary electrons can escape from all points of the grain. Thus, δ for spherical dust grain is very higher than that determined by Sternglass equation.

In this work, size dependent yield equation derived by Chow, Mendis and Rosenberg (1993) for the enhanced secondary emission yield from a very small spherical dust grain is used. The study on charging of small dust particle is of fundamental interest, for it allows for the coupling between the fields and particles environment to the dynamics of the dust grains. Charging during SEPs could prove even more hazardous because of the enhanced charging and radiation dosage (Jejcic et al., 2014)

In Section 2 we describe the nature of data that we use for the present work and explain how the theory is derived to calculate the charging currents. We present our results and discuss the role of grain radius in dust charging in Section 3 and Section 4 contains conclusions and future prospects.

2. Data and theory

2.1 Data

We used the electron concentration (n_e) and temperature (T_e) measured by the Electron Reflectometer aboard Lunar Prospector (LP) spacecraft (courtesy PPI data service of NASA). The LP orbited around the Moon in 1998-1999 and was designed for a low polar orbit investigation of the Moon, including mapping of surface composition and possible deposits of solar ice. Electron Reflectometer provides the electron data from 7 eV to 20 keV, with its altitude varying 30 and 115 km. Data from 19 months mission help to improve the current understanding of the Moon. The mission ended on 31st July 1999 when the spacecraft impacted the Moon near the South Pole in a controlled crash to look for the evidence of water ice. The LP observes the largest negative lunar surface potentials during plasma sheet crossings and SEP events, when the Moon is exposed to energetic plasma. The LP Electron Reflectometer (ER) was designed to map lunar crustal magnetic fields but also found evidence for lunar electric fields (Halekas et al., 2008). For adiabatic magnetic reflection, the cutoff pitch angle α_c (the angle between the initial electron velocity and the magnetic field beyond which electrons impact the lunar surface before reflecting) measured at the spacecraft is given by $\sin^2 \alpha_c = B_S / B_M$. In the absence of parallel electric fields, the loss cone boundary does not depend on electron energy. However, when a potential difference exists between the surface and LP, this loss cone has a characteristic variation with energy. The energy dependence of the loss cone modified the loss cone angle equation to read $\sin^2 \alpha_c = \left(B_S / B_M\right)\left(1 + e\Delta U / E\right)$, where E is the electron kinetic energy measured at the spacecraft and ΔU is the potential difference between the surface and the spacecraft and the method of determining the surface potential using loss cone angle was detailed in Halekas et al. (2008).. During solar energetic particle events and in the terrestrial plasma sheet, nightside potentials of up to $-4.5\ kV$ are possible (Halekas et al., 2007; Halekas

et al., 2008). Halekas et al. (2008) reported a massive SEP event on 6 May 1998. Data is collected when the space craft was in wake region and was at an altitude of about 100 km above the surface (Figure 1). The activity maxima observed at 08:00 UT and during the event, the measured electron energy is 1000 eV. Only a few electrons ($n_e = 0.002cm^{-3}$) can reach the wake region because of the existence of large negative potential. This is the reason for decrease in n_e and increase in T_e.

2.2 Dust grain charging in plasmas

Dust particles immersed in plasma collect electrostatic charges and respond to electromagnetic forces in addition to all the other forces acting on uncharged grains. The study on charging of small dust particle is of fundamental interest, for it allows for the coupling between the fields and particles environment to the dynamics of the dust grains. Once dust particles are knocked off the surface, either from meteoritic impacts, electrostatic levitation or human activity, their charges readjust to the ambient plasma conditions (Horanyi et al., 2015).
In this section we discuss the charging theory of levitated isolated grains above the lunar surface in plasma and derive equations for lunar dust charging during SEPs in the nightside region. The lunar dust charges in response to incident current. The main sources of charging currents are i) plasma electrons (I_e), ii) plasma ions (I_i) and iii) secondary electrons (I_s). I_s arises mainly due to the bombardment of highly energetic electrons. Total current to the dust grain immersed in the plasma is

$$\frac{dQ}{dt} = I = I_e + I_i + I_s = \sum_k I_k \tag{1}$$

The grain immersed in plasma reaches to a floating potential such that the net current incident on it is zero, i.e.

$$\sum_k I_k = 0 \tag{2}$$

These currents depend on plasma parameters (density, temperature, energy distribution) and dust grain properties (size, surface potential). We assumed the plasma with the Maxwellian energy distribution corresponding to temperature T and electron and ion densities, n_e and n_i respectively and that $n_e \sim n_i$ as there is no ion data available.

2.2.1 Charging theory of isolated dust grains in Plasma

The flux of electrons and ions moving in z direction with velocity v_z , bombarding an isolated dust grain with radius a , $a << \lambda$ (Rao, Shukla and Yu, 1990),

$$\Gamma_\alpha = \int v_z f_\alpha(v) d^3v \tag{3}$$

can be evaluated by integrating the velocities in spherical coordinates (v, θ, ψ), with the velocity volume element given by

$$d^3v = v^2 dv \sin\theta d\theta d\psi \tag{4}$$

Here $\alpha = e$ for electrons and $\alpha = i$ for ions, λ is the Debye screening length and $f_\alpha(v)$ is the distribution function which is given by

$$f_\alpha(v) = n_\alpha \left(\frac{m_\alpha}{2\pi K T_\alpha} \right)^{3/2} \exp\left(\frac{-E}{K T_\alpha} \right) \tag{5}$$

where K is the Boltzmann constant.
Substitute Equations (4) and (5) in Equation (3)

$$\Gamma_\alpha = \int_{v=0}^{\infty}\int_{\theta=0}^{\pi/2}\int_{\psi=0}^{2\pi} v\cos\theta f_\alpha(v)v^2\sin\theta d\theta d\psi dv$$
$$= \pi\int_0^{\infty} v^3 f_\alpha(v)dv \tag{6}$$

and equation for current

$$I_\alpha = 4\pi a^2 e\int_0^{\infty}\pi v^2 v f_\alpha(v)dv \tag{7}$$

Electron current,

$$I_e = -4\pi a^2 ne\left(\frac{m}{2\pi KT}\right)^{3/2}\frac{2\pi}{m^2}f_1(\varphi) \tag{8}$$

where

$$f_1(\varphi) = \int_{-e\varphi}^{\infty} E\exp\left(\frac{-E}{KT}\right)(1+\frac{e\varphi}{E})dE$$
$$= (KT)^2\exp\frac{e\varphi}{KT} \tag{9}$$

where φ is the lunar dust potential. For $\varphi < 0$, Equation (8) becomes

$$I_e = -4\pi a^2 ne\left(\frac{KT}{2\pi m}\right)^{1/2}\exp\frac{-e\varphi}{KT} \tag{10}$$

Similarly,

$$I_i = 4\pi a^2 ne\left(\frac{m}{2\pi KT}\right)^{3/2}\frac{2\pi}{m^2}f_2(\varphi) \tag{11}$$

where

$$f_2(\varphi) = \int_{e\varphi}^{\infty} E\exp\left(\frac{-E}{KT}\right)(1-\frac{e\varphi}{E})dE$$
$$= (KT)^2(1+\frac{e\varphi}{KT}) \tag{12}$$

For $\varphi < 0$, Equation (11) becomes

$$I_i = 4\pi a^2 ne\left(\frac{KT}{2\pi m}\right)^{1/2}(1+\frac{e\varphi}{KT}) \tag{13}$$

2.2.2 Secondary electron current

At very high electron energy, some of the bombarding particles are energetic enough to ionize the dust grain and produce the secondary electron. The escape flux of the secondary electrons represents a positive charging current. The ratio of the emitted secondary electrons to incident ones is a function of the incident electron's energy and radius of the dust grain and is called secondary yield (δ) .

Secondary electron current can be calculated by integrating the energy differential flux of the primaries with the secondary yield.

$$I_s = 4\pi a^2 ne\left(\frac{m}{2\pi KT}\right)^{3/2}\frac{2\pi}{m^2}\int_{-e\varphi}^{\infty} E\exp\left(\frac{-E}{KT}\right)\left(1+\frac{e\varphi}{E}\right)\delta_{(E,a)}dE \quad (14)$$

The main difference of this work and already published results (Horanyi, 1996) is the adoption of the yield equation of Chow, Mendis and Rosenberg (1993).

$$\delta_{(E,a)} = \frac{1}{2}\int_0^{\min\left(D_g, x_{\max}\right)} K_s K_w (E^2 - K_w x)^{-1/2} f(x)dx \quad (15)$$

where

$$f(x) = \frac{1}{2}\int_0^{\pi} \exp(-\beta l(x,\theta)\sin\theta d\theta \quad (16)$$

Here D_g is the diameter of the dust grain, K_s represents the efficiency with which the lost primary electron energy is used to excite the secondary's, K_w is the Whiddington's constant (Whiddington, 1912), β is the inverse of the absorption length for secondary's, $l(x,\theta)$ is the distance that a secondary electron must travel to reach the surface from a depth x and along an angle θ from the primary electron path (as shown in Figure 2). Since a primary electron ejects secondaries along the entire path within the grain, Equation (15) must be integrated from the point of entry ($x = 0$) to either the point of exit $x = D_g$ or the maximum penetration distance ($x_{\max}$), depending on which among them is smaller. The maximum penetration depth corresponds to the point at which $E(x) = 0$ and can be determined from Whiddington's law as, $x_{\max} = E^2 / K_w$. From Figure 2 we geometrically solve $l(x,\theta)$.

$$l(x,\theta) = \left\{a^2 + (a-x)^2 - 2a(a-x)\cos\theta'\right\}^{1/2} \quad (17)$$

where

$$\cos\theta' = \cos\theta\sqrt{1-\left(\frac{a-x}{a}\right)^2\sin^2\theta} + \left(\frac{a-x}{a}\right)\sin^2\theta \quad (18)$$

Substitute Equations (15), (16) and (17) in Equation (14) to get secondary electron current.

Dust grain will reach a floating potential such that the net current incident on it is zero. So to find the equilibrium surface potential of dust grains we need to numerically solve the current balance equation, Equation (1), after including the electron, ion and secondary electron current.

$$-ne\left(\frac{KT}{2\pi m}\right)^{1/2}\exp\frac{-e\varphi}{KT} + ne\left(\frac{KT}{2\pi m}\right)^{1/2}\left(1+\frac{e\varphi}{KT}\right) + ne\left(\frac{KT}{2\pi m}\right)^{1/2}\exp\frac{-e\varphi}{KT}\delta_{(E,a)} = 0 \quad (19)$$

Equation (19) was numerically solved to get negative dust grain potential during SEPs.

3. Results and Discussions

SEP events are always associated with events taking place at the Sun, such as flares, filament disappearances and Coronal Mass Ejections (CMEs) (Lario, 2005; Gopalswamy et al., 2004). The peak obtained on LP data (Figure 1) at 08:00 UT was due to the high energy electron fluxes associated with the SEP event. Charging currents and equilibrium surface potential for lunar dust grains under SEPs were calculated using electron data from LP spacecraft. The role of grain size during its charging is discussed in detail in this study.

3.1 Secondary yield and grain radius

We numerically solved Equation (15) to study the variation of secondary yield as a function of primary electron energy, E for different sized conducting dust grains (Figure 3). The parameter values used for β, K_w and

K_s are $0.93\times10^{6}cm^{-1}$, $0.42\times10^{12}\ eV^{2}cm^{-1}$ and 0.04, respectively. As electron energy increases, yield value also increases and reaches to a maximum value. Further increase in energy decreases the yield. At low primary energies the smaller dust grains have higher yields, because in smaller grains the excited secondary electrons have shorter distance to travel to reach the surface. When the primary electron energy exceeds $E_{\min}=\left(K_w D_g\right)^{1/2}$, the electrons tunnels right through the grain and does not excite as many secondaries as a primary that is stopped within the grain. However, as the primary energy increases, the yield curves for different sized grains cross each other and at very high energy larger grains show higher yields than smaller ones. The reasons are: 1) larger grains will have a larger upper limit of integration in Equation (15), 2) for smaller grains the time of impact is too small to eject the secondary electrons and 3) after 600 eV, the value of $x_{\max}\approx0.8\ \mu m$ and so the electron tunnels through $0.5\ \mu m$ grain without producing much secondaries than in $1\ \mu m$. For $0.5\mu m$ dust grain the maximum yield value (δ_m) is 2.3 and for $1\mu m$ grain it is only 1.8. All grains show a maximum yield at 550 eV which is in well agreement with lunar sample experimental observation (Anderegg et al., 1972). As the electron energy reaches 1200 eV, δ_m for smaller grain is 0.8, but for larger grain it is well above 1. We get an optimal yield value of 1.75 at 650 eV where two yield curves cross each other. After the optimal value, yield values of smaller grains vary very rapidly with electron energy.

In the work, we used an yield equation that depends on the radius of the grain. Figure 4 compares our result and the yield obtained by Sternglass (1957), where the yield has no dependence on the grain size. The yield of secondary electron emission is significantly higher in our model than in Sternglass (1957). This is because of the increase in secondary electrons which can escape from all parts of the grain. For $0.5\mu m$ grain the calculated yield value is 2.3, but for Sternglass model the yield value is only 1.5. Also at very high energy values, $\frac{d\delta}{dE}$ variation is not predominant in Sternglass model.

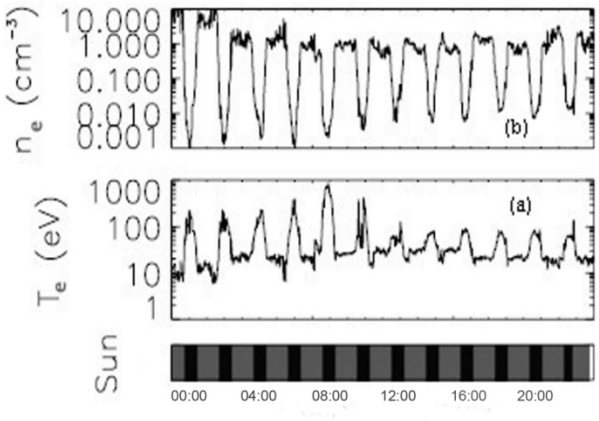

Figure 1: Lunar Prospector spacecraft data from ElectronReflectometer on 6 May 1998 (a) Electron temperature data, (b) Electron number density data and color bar showing spacecraft illumination (black=shadow, grey=sun) for a series of orbits in the solar wind and lunar wake during SEP event on 6 May1998.

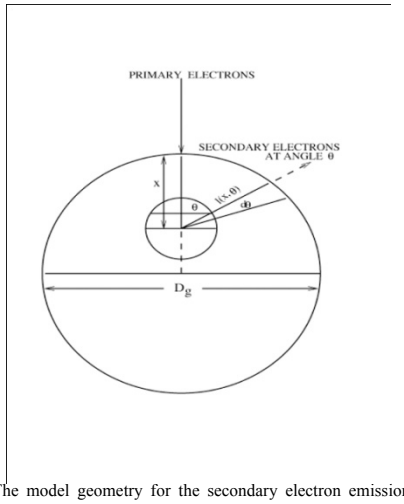

Figure 2: The model geometry for the secondary electron emission from a small spherical dust grain of diameter D_g.

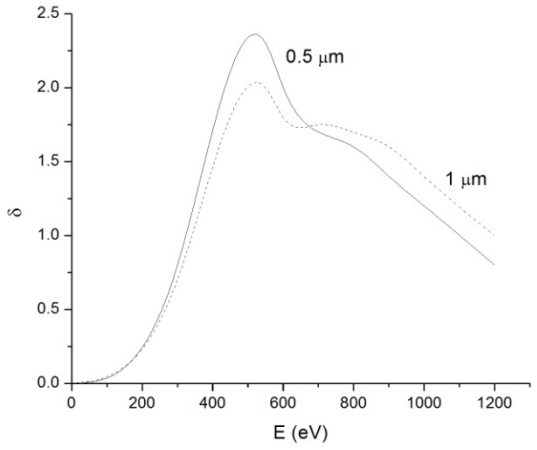

Figure 3: Variation of secondary yield as a function of primary electron energy (E) for different sized conducting grains (0.5 μm , 1 μm).

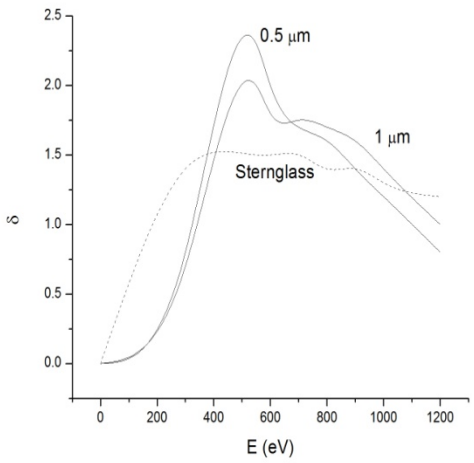

Figure 4: The curve of yield (δ) values against primary electron energy (E) and comparison with Sternglass model.

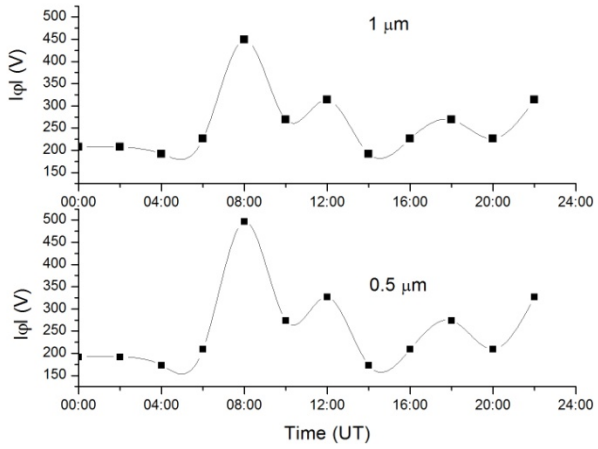

Figure 5: The time plot of surface grain potential of different grain radii (0.5 μm , 1 μm) during SEP events. Peaks are obtained when the solar activity is maximum.

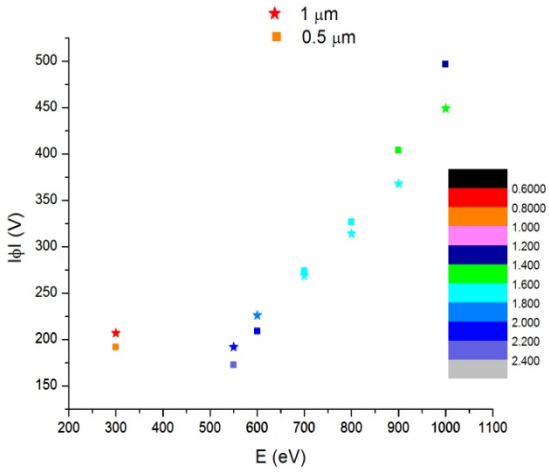

Figure 6: Variation of grain potential with electron energy and showing the dependence of secondary yield on grain potential during SEP events.

3.2 Grain potential and electron energy during SEPs

A strong dependence of secondary electron emission on grain size results in the different equilibrium surface potentials for grains of different radii. Negatively charged grain enhances the ion flux and lowers the electron flux. The grain reaches an equilibrium surface potential where a sum of all currents to the grain is zero.

Figure 5 explains the time plot of lunar dust potential during SEPs for $0.5\mu m$ and $1\mu m$ dust grains. The peaks are obtained at the time when the solar activity is maximum, i.e., when the energy of the incident electron is high. In both cases the potential is more than -400 V. During enhanced solar activity time smaller grains show large negative potential than larger grains. A $0.5\mu m$ grain shows -497 V potential, whereas $1\mu m$ grain has only -449 V. This is because of the large secondary yield shown by grains with large radii. One could expect a positive potential if the yield exceeds unity. However, here negative potential was obtained at all temperatures. The reason is that, because

of large negative potential, the role of secondary electron current is only to decrease the magnitude of negative potential during SEPs. Figure 6 included the dependency of grain radius and yield on equilibrium grain potential for different energy values. At energy $E = 1000$ eV, yield value of larger grains ($\delta = 1.4$) are greater than that of smaller grains ($\delta = 1.2$). The reason is, at very high energies secondary electron current exceeds the negative electron current for large grains. Secondary electron current is equivalent to an incident ion current, which decreases the negative potential of large grains. Secondary yield of large grain is low for small electron energy and as a result they charge to a large negative value. Charged dust grains can levitate above the lunar surface if, the repulsive electrostatic force between dust and the surface is sufficiently large to overcome the gravitational force on the grain (Stubbs, Vondrak and Farrell, 2006). However, during SEPs electrostatic force experienced on dust grain is sufficient large to levitate to a large distance thereby causing serious threat to the lunar exploration activities.

4. Conclusions and future prospects

Lunar surface charging and lunar dust charging are two important regimes where we need to focus much for the safe operation of our future lunar missions. We developed a theory to discuss how a single isolated dust particle collects its electrostatic charge due to the various incident electron currents and reach to a floating potential. We used an yield equation which depends on grain radius for calculating the secondary electron current. The true secondary yield was considered in the theory and the contribution of back scattered electron was ignored as their energies are lower than that of primaries. Using the derived theory and space craft data we calculated the various charging currents and equilibrium surface potential for lunar dust grains of different radii during SEP events. Our calculation show variances of the equilibrium surface potential with the grain size, especially during SEP events. This is caused by an enhancement in the secondary electron current under high electron temperatures. Our yield value is very high than the previous calculation based on classical Sternglass (1957) equation. During SEPs because of very high electron temperature, $1\mu m$ grain shows a potential of -449V.

Dust particles are continuously adjusting their surface potential towards the local equilibrium value as influenced by the charging plasma conditions. The fields and particle environment can uniquely shape the size and the spatial distribution of the dust grains. Studies of the motion of charged dust particles connect a number of phenomena that are often thought to be unrelated. The electric field of these lofted dusts may interact with the field of equipment onboard the spacecraft and damage its functioning. So space missions are designed to make simultaneous in situ and remote observations and need to include devices like plasma detector that can provide the useful data of composition, density and energy density of the plasma. These data are used to calculate the charging currents of the grains and to determine the equilibrium dust potential.

In summary,

1) The electron energy corresponds to maximum yield value obtained by using the derived theory agrees well with the experimental observation.
2) Lunar dust charging varies significantly with grain radii during SEP events.
3) Secondary yield value for spherical dust grains are very large than that calculated by using Sternglass equation. At low primary electron energy, small grains show large yield values and as temperature increases, larger grains show high yield values.
4) Small grains show large negative potential during SEP events.

Acknowledgements: One of the authors (S.B.R.C.) acknowledges the financial assistance under the scheme on Minor Research Project of the University Grants Commission, Government of India (1709-MRP/14-15/KLKE001/UGC-SWRO). We would also like to acknowledge Planetary Plasma Interaction (PPI) data service for providing electron data from Lunar Prospector spacecraft. Figure 2 reproduced courtesy of Chow et al.,1993.

References

Anderegg M, Feuerbacher B, Fitton B, et al., Secondary electron emission characteristics of lunar surface fines, Proc. Lunar Sci. Conf. 3rd, 1972, 2665.

Cain JR, Lunar dust: The hazard and astronaut exposure risks, Earth Moon Planets, 107, 2010, 107-125.

Chow VW, Mendis DA and Rosenberg M, Role of grain size and particle velocity distribution in secondary electron emission in space plasmas, J. Geophys. Res., 98, 1993, 19065-19076.

Colwell JE, Batiste M, Horanyi M, et al., Lunar surface: Dust dynamics and regolith mechanics, Rev. Geophys., 45, 2007, RG2006.

Criswell DR, Horizon glow and the motion of lunar dust, in Photon and Particle Interactions with Surfaces in Space, RJL Grard (Ed.), D. Reidel Publishing Co., Dordrecht, Holland, 1973, 545-556.

Gopalswamy N, Yashiro S, Krucker S, et al., Intensity variation of large solar energetic particle events associated with coronal mass ejections, J. Geophys. Res., 109, 2004, 2156.

Halekas JS, Delory GT, Lin RP, et al., Lunar Prospector observations of the electrostatic potential of the lunar surface and its response to incident currents, J. Geophys. Res., 113, 2008, A09102.

Halekas JS, Delory GT, Brain DA, et al., Extreme lunar surface charging during solar energetic particle events, Geophys. Res. Lett., 34, 2007, 1-5.

Horanyi M, Charged dust dynamics in the solar system, check Annu. Rev. Astron. Astrophys.,34, 1996, 383-418.

Horanyi M, Walch B, Robertson S, et al., Electrostatic charging properties of Apollo 17 lunar dust, J. Geophys. Res., 103, 1998, 8575-8580.

Horanyi M, Szalay JR, Kempf S, et al., A permanent, asymmetric dust cloud around the Moon, Nature, 522, 2015, 324-326.

Jejcic S, Heinzel P, Zapior M, et al., Multi - Wavelength eclipse observations of a quiescent prominence, Solar Phys., 289, 2014, 2487.

Lario D, Advances in modeling gradual solar energetic particle events, Adv. Space Res., 36, 2005, 2279-2288.

RakeshChandran SB, Renuka G, Venugopal C, Plasma electron temperature variability in lunar surface potential and in electric field under average solar wind conditions, Adv. Space Res., 51, 2013, 1622-1626.

Rao NN, Shukla PK and Yu MY, Dust - acoustic waves in dusty plasmas, Planet. Space. Sci., 38, 1990, 543-546.

Rennilson JJ and Criswell DR, Surveyor observations of lunar horizon glow, The Moon, 10, 1974, 121-142

Sternglass EJ, Theory of secondary electron emission by high - speed ions, Phys. Rev., 108, 1957, 1-12.

Stubbs TJ, Vondrak RRand Farrell WM, A dynamic fountain model for lunar dust, Adv. Space Res., 37, 2006, 59-66.

Whiddington R, The transmission of cathode rays through matter, Proc. R. Soc. London, 86, 1912, 360.

Whipple EC, Northrop TG, Mendis DA, The electrostatics of a dusty plasma, J. Geophys. Res., 90, 1985, 7405-7413.